Spectroscopic analysis of quasar absorption lines

MS.Anamitra Kundu[1], Dr Jyoti Singh[2], Dr.Katherine Rawlins[3]
[1]*Department of Physics, St. Xavier's College (Autonomous), Mumbai*
[2]*Mentor, Head of the Department Associate Professor, Department of Physics, St Xavier's College, Mumbai*
[3]*Guide, Assistant Professor, Department of Physics, St Xavier's College, Mumbai*

Abstract- This thesis is entitled to have an understanding about the evolution and galaxy formation where the knowledge of atomic and ionic states and their role in star formation. Being highly luminous and independent in understanding the gas content in distant galaxies, absorption-line spectroscopy of quasars helps in doing a clear analysis for the star formation. This thesis presents the study of metal absorption lines in QSO J000443-555044 and determining the Equivalent Width to find the strength of the absorption lines. QSO J000443-555044 is an unnormalized spectrum, which is normalized and fitted to get the Equivalent Width. We also look to find the velocity of the observed lines which shows prominent features to understand whether all the absorption lines belong to the same absorbing cloud.

INTRODUCTION

To understand the universe and its evolution is one of mankind's great interests. Over the last decades science have made significant progress in understanding the galaxy formation and evolution through the use of observations and models. In the 1950's Guido Munch observed metal ions like neutral sodium and singly ionized calcium in the spectra of hot stars where there are high galactic latitudes. Before publishing the data in (Munch & zirin et al, 1961) he and Spitzer concluded that the lines observed show diffuse extrapolar hot gas which have a temperature around 10^6.

From the above theory, the idea of "Galactic Corona" and its exploration with the help of absorption lines in the spectra of background objects came into view. Based on this idea after the discovery of quasars in 1963 it was proposed that most of the absorption lines that are observed in the quasi-stellar media have multiple absorption redshifts, due to the presence of gas in the extended halos of normal galaxies. In the research to follow, theorists found that it was impossible to have an idea about the galaxies without knowing about the gas flows and the implication of CGM.

Quasar spectra has its importance because it provides a large amount of astrophysical information about galaxies. Features like the absorption of the metal line transition and analyzing the oscillatory strength, and distinguishing between a strong or a weak absorber of the absorption lines could be analyzed.

Here, we review and try to find the information about these quantities for 38 transitions in the QSO J000443-J000443 which are of Si, Mg, Al,Cr, Fe, Ni and Zn.

1.1 Circumgalactic Medium (CGM)

The CircumGalactic Medium (CGM), is the region around a few hundred kiloparsecs from a galaxy containing an enormous and extended reservoir of diffuse gas. The current research in understanding galaxy evolution has changed significantly with the new understanding of the role of CGM and its importance in star formation. The CGM also acts as a major reservoir of baryons in a galaxy and is actively regulating galaxy evolution.

CGM can be studied both by observation and by simulations extensively by using Hubble Space Telescope (HST) and ground based large telescopes such as Very Large Telescope (VLT), Keck, Gemini to understand the impacts of CGM over galaxy evolution. Here we have used the European Space Observatory (ESO)'s VLT to analyze an QSO spectrum J000443-555044.

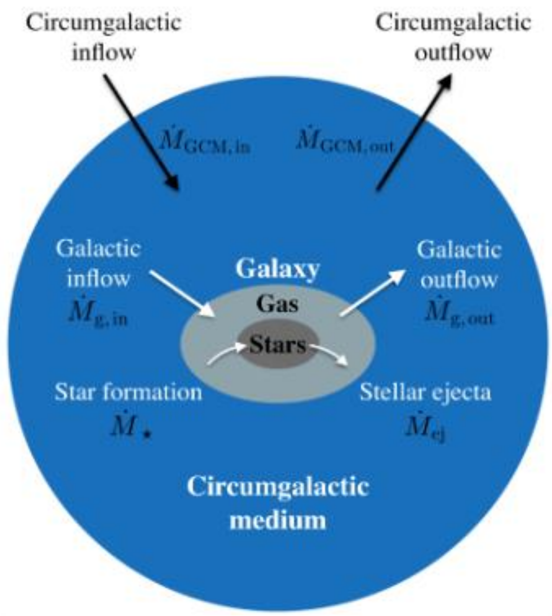

Figure 1.1 Schematic Representation of CGM

1.2 CGM and its importance in Galaxy formation and Evolution

Studies show that in recent years the CGM forms the main constituent of galaxies and has an important role in our understanding of galaxy evolution due to the modern research in observational studies through which we can learn more about this diffuse , nearly invisible material. Observations and simulations of this constituent of galaxies suggest that it is a multiphase medium having rich dynamics and complexity in its ionization states. CGM is a source of a galaxy's star-forming fuel, andalso most likely the main regulator of the galactic gas supply.

1.3 How to study a CGM through Absorption Lines

Observing and analyzing The CGM which have bright background source and near to Quasar absorption lines have great benefits rather than using the other methods observed due to the following. a) The sensitivity to extremely low column densities, b) Can be searched for a wide range of densities and lastly,c) the uniformity of the detection limit to the redshift and the luminosity of the host galaxy. It is also observed that there is a chance of using multiple sightlines as observed in (Lehner, Howk & Wakker,2015, and Bowen et.al, 2016.)

It is both easier and helpful in identifying The H1 column density which can be use differently in analysis. LInes upto logN ~ 15 can easily be identified with equivalent widths or Voigt profile fitting. The values higher to logN ~15 will be high for the Lyman -alpha forest but low for CGM(there are of course a few exceptions,(Tumlinson et al,2013 Johnson et al ,2014)b where H1 is not seen at < 100 kpc even to low limits. When logN ~ 16 , saturation becomes a major factor and shows high column density(as opposed to lower limits) , it must come from profile fitting or from the higher Lyman lines, having maximum redshifts. Systems having logN ~16 form a partial or complete Lyman Limit System.

If the Lyman Limit is covered (z > 0.24 for Hubble), the flux decreases at λ=912(1+ z) Å which shows an accurate measurement of $\log N_{H1}$ and an improved ionization and metallicity. Systems having greater to $\log N_{H1} \sim 18$ (where N_{H1} is the H1 column density in cm^{-2}), the Lyman limit remains opaque , the highest Lyman series lines will and the original column densities can be observed by fitting the Lyman alpha profile for both LLS and DLAs.

1.4 Physical State of the CGM

To draw conclusions from the different observations made till date the CGM is "multiphase" when it is at its ionization structure and becomes complex in it's dynamics, as shown in the figure 2 (Tumlinson et.al,2013)which represents a range of ion equivalent width (rest frames) measurements.

There is clear proof of the complexity present , and the different ion species which break into different components having distinct velocities and linewidths. Fitting Voigt profiles to multicomponent absorption yields column densities N , Doppler b parameter, and thew velocity offset v for each component from the galaxy systemic redshift, as well as the total kinematic spread of gas. This will be elaborated further in the later contents of this work.

2.1 Absorption lines

An absorption line is observed in a spectrum , when an absorbing material is in between the source and the observer. The material could be present anywhere, be it in the outer layers of astar a cloud of interstellar gas or a cloud of dust. Based on the quantum mechanics theory, an element, atom or a molecule will absorb photons which have energies equal to the difference between two energy states.

Based on this feature of the atom it can absorb electromagnetic radiation but not the electromagnetic radiation of arbitrary wavelength or arbitrary color.In that way each atom will be different. Absorption lines are observed as dark lines , or lines where the intensity is less on a continuous spectrum which is usually observed where there is an abundance of hydrogen gas in the outer layers of the star which is going to absorb some of the light from the underlying thermal blackbody spectrum.

A good example is that of the neutral hydrogen which absorbs wavelength of 1215.67,1025 A which is not possible in any other atoms to have precise measurement. If in case the absorption observed is negligible, we should be able to have an accurate measurement of the width, secondly a very accurate value for the doppler broadening parameter and lastly the velocity should be distributed with respect to a single Gaussian.

2.1.1 Optical Depth and curve growth

A. For stars like the sun the weak absorption lines are replaced by Doppler Broadening, where the width of the line is caused by random motions of the atoms absorbing the light. The broadening is directly proportional to the number of absorbing atoms.

By the definition of optical depth,

$$\frac{I}{I_0} = e^{-\kappa \rho s} = e^{-\tau}$$

Here, the density, ρ is directly proportional to the optical depth, which affects the equivalent width. For thermal broadening, we need to learn the absorption profiles. Three profiles can be concluded from here. First, the increase in the optical depth increases the equivalent width of the line as there is a linear relation between the number of atoms and equivalent width, for optically thin line. Second, when the line grows thicker the equivalent width does not grow with the optical depth , i.e with the number of atoms and finally reaches a saturated state. Third, with very optically thin lines, the equivalent width due to thermal motion grows very slowly, and the equivalent width increases in the wings of the depth. The wings of the line are caused due to atoms which are moving either towards or away from the observer. All these three regimes are observed as shown in the following fig1.2 (referred from Draine,2018).

From the figure 1.2 we observe that the dip is optically thin and narrower compared to the second profile where the deposition of the metal had reached its saturated state. Lastly as there is no place of deposition vertically down due to its saturated state, the deposition is taking place sideways forming wings.

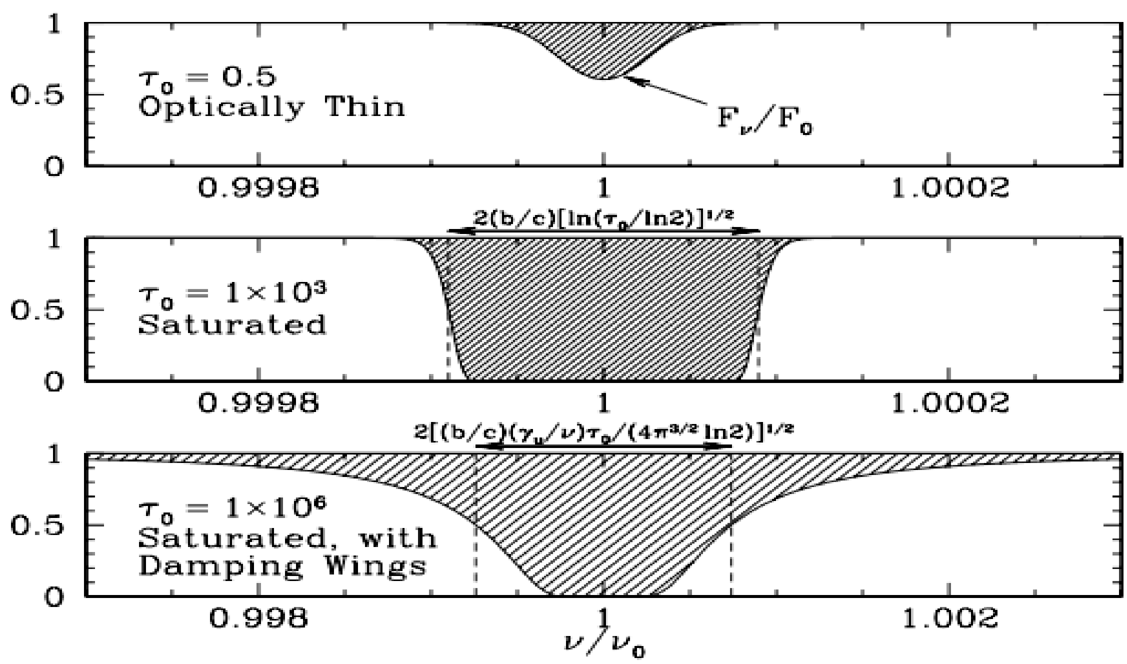

Figure 1.2 Absorption profiles observed in the regimes.

2.2 Quasar Absorption lines

Quasars are distant galaxies with active nuclei. We could in fact observe only the nucleus as the rest of the galaxies are too faint to be observed at large distances. Quasars emit energy in a wide spectrum of electromagnetic radiation. The light contains all possible colors.

As discussed before in section 2.1, the clouds consisting of atoms and ions would absorb certain wavelengths by determining the position of the redshifts. Thus quasars coming in contact with the gas will show a distinct absorption profile, on the continuum that is dependent on densities and temperature which is represented in fig 3 taken from the reference (John Webb, 2004).

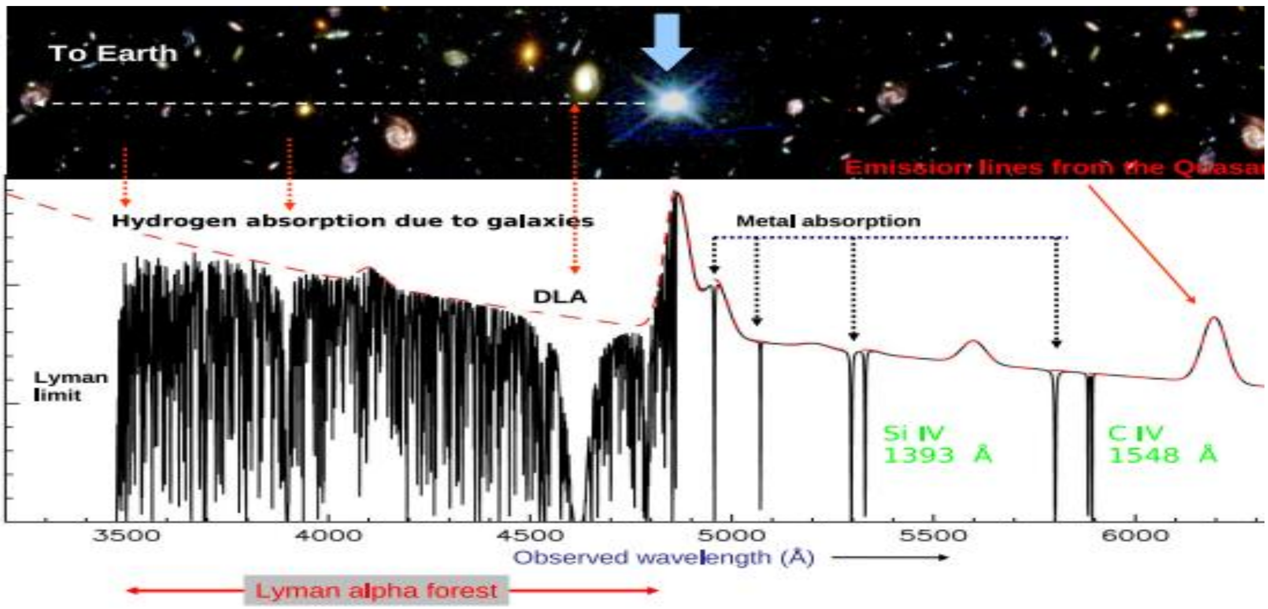

Fig 1.3 : A representation of the quasar absorption line showing the absorption,along the quasar (John ,Webb,2004)

2.2.1 Lyman-α Absorption in Quasar Spectra

The broad emission peak at ~ 3700 A from the Fig 4 represents the Hydrogen emission from the quasar and the strong Hydrogen absorption line at ~ 3500 Å is produced by an intervening galaxy. Our aim is to observe and analyze the metal absorption lines which belong to the same observer, which gives rise to the Lyman- alpha dip. Most of the Hydrogen lines seen, as most of the neutral Hydrogen atoms are in the ground state, are from the Lymanseries transitions. The most common of these transitions seen in quasar spectra is the Lyman-α transition ($n = 1 \rightarrow 2$) at 1215.6701 Å (the strongest of the series). Different absorption systems can be broadly classified into four categories (Table 1.1) based on their neutral Hydrogen column densities, derived from the Lyman α lines.

Table 1.1. The classification, based on NHI , of absorption systems seen in quasar

Column Density	Classification
$\log N_{HI} < 17.2$	Lyman- alpha Forest
$17.2 <= \log N_{HI} <= 19.0$	Lyman - Limit- System(LLS)
$19.0 <= \log N_{HI} <= 20.3$	Sub - Damped Lyman- alpha
$20.3 <= \log N_{HI}$	Damped- Lyman alpha

2.2.2 Detection of the absorption lines

According to the current research different type of absorbers give rise to these absorption lines, whereas the majority of Ly alpha and higher series are formed in the Ly alpha clouds which is recently believed to be metal deficient.Due to the present of high neutral column densities which are known as lyman limit systems(LLs) that are optically thick for Lyman continuum photons.(lamda< 912 A in the absorber rest frame) and produces sharp edges in the quasar spectra, which at times completely absorbs the quasar flux below(1+z)912 A where z is the redshift of the absorber. Majority of strong metal lines fall into the ultraviolet frequency range, even if originating at higher redshifts. The successful implementation of the Hubble Space Telescope (HST). In the recent trailblazing observations with the ESO's Very Large Telescope (VLT) at Paranal leading strong support to current computer models of the early universe. In recent years it has provided a substantial breakthrough in the studies of QSO absorption lines. Yet, due to the LLS mentioned above only a few quasars are known to exhibit detectable flux over a wide range of the UV part of the electromagnetic spectrum.

2.2.3 Damped Lyman Alpha System (DLAs)

Damped lyman alpha is based on the concentrations of neutral hydrogen gas that is observed on a quasar spectrum. These systems are observed in high redshifts ranging from 1.5 - 4. The observed spectra consist of neutral hydrogen Lyman alpha absorption lines which are broadened by radiation damping. As these systems are observed in absorption and not in the emissions of their stars, they provide an opportunity to study the dynamics of the gas in early galaxies directly.

By definition, due to the presence of high H1 column densities , they shield the gas from ionizing radiation thus making it highly neutral.

As DLAs contain large amounts of universal metals, studying their chemical abundances and metallicities and how these evolve with redshift are therefore important elements in understanding galaxy formation and evolution. DLA metal abundances and metallicities can be very accurately measured, owing to the simple relationship between optical depth and column density, and the neutrality of the DLA gas . The most accurate and precise DLA metal-line measurements are possible in high-resolution spectra because the metal line velocity structures can be resolved.

To assist such work we have used the DLA spectrum J000443-555044 in our study, as analysis of this sightline has not been reported in detail in literature.

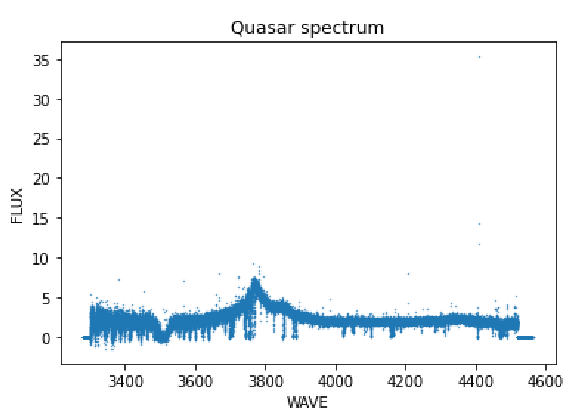

Fig 1.4 : The un-normalized observed QSO J000443-J000443 spectrum

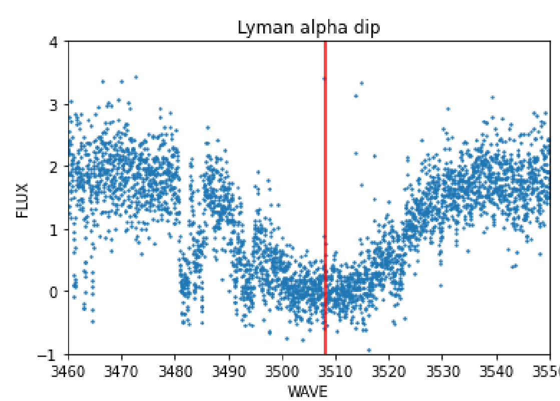

Fig 1.5 : Zoomed Lyman -alpha dip

Fig 1.5 represents the entire QSO spectrum. As we are not taking the entire spectrum into our consideration we zoom into the region of the Lyman - alpha dip. Fig 5 illustrates the observed Lyman alpha dip after zooming.

ESO Phase 3 Data Release Description Of QSO - J000443-555044

Our sample QSO J000443-555044 is observed to have zabs = 1.88. This is the release of reduced 1D spectra from the UVES 1 spectrograph, ECHELLE mode . The selected data cover the vast majority of the entire UVES data archive, from the beginning of operations in March 2000 until present. Whenever applicable stacked spectra have been generated.

For the UVES data until 2015-06-30, the master calibrations have been reprocessed using the same pipeline version as used for the scientific products. From the ESO site it is observed that they have used a two-step processing scheme. In the first step, for consistency all single exposures are processed with the UVES pipeline 5.10.13 and higher (recipe uves_obs_scired). All data have their instrument signature removed (de-bias, flat fielded), with the exception of the absorption of the data which have the signature of the iodine cell removed. Thus the UVES pipeline will be biased, flat-fielding in an automated way.

As these data products are considered to be ready for scientific analysis, as mentioned in the ESO documentation of the spectrum , we use them to do the line profile studies and radial velocity studies, by observing the Equivalent width.

3.1 Data Selection and Analysis:

The data downloaded are with their archive names . The README file along with the downloaded contains the information that is necessary. The file is properly renamed by replacing column 2 in the ADP file which is the technical name and column 3 whose original name starts with UV.

After converting the ADP file to CSV the redshifted frequency will be converted to the rest frame wavelength for spectral analysis. These spectras will then be normalized to the continuum level using the best fit lines.

We searched for a total of 38 lines, out of which we observe that Si II 1808, is a prominent absorption line, and hence it is taken as a reference line to observe the other line profiles. We consider and measure the Equivalent Width of those lines having similar shape and dip at the same velocity as Si II 1808 and use it for identification. With reference to it we observe the equivalent width for Al III 1854, Al IIi 1863, Al III 1670, Fe II 1608, Cr II 2056, Zn II 2026, Ni II 1393, S I 1295, Si II 1256.

B II 1335.53	Mg II 1240.40	SIII 1190.20
C II 1335.71	Mg II 1239.93	Fe II 1608
C II 1335.71	Si II 1808	Fe II 1260.53
C IV 1548.20	Si II 1526.71	Fe III 1214.56
N I 1200.71	Si II 1304.37	Co II 1552.76
N I 1199.55	Si II 1260.42	Co II 1480.95
NV 1238.82	Si II 1193.29	Co II 1466.21
NV 1242.80	Si II 1190.42	Co II 1424.79
O I 1355.60	S I 1473.99	Ni II 1502.15
O I 1302.17	S I 1295.65	Ni II 1467.76
Ni II 1467.26	Ni II 1454.84	Ni II 1393.32
Al III 1854	Al III 1670	Fe II 1608
Zn II 2026	Cr II 2056	

Table 1.2 : List of Metal Absorption Lines

3.2 Observing the Profile Fitting, Normalization of the observed Absorption Lines

3.2.1Continuum fitting and Normalization.

3.2.1a Continuum fitting:

Continuum fitting is done to compare the fit of the spectrum image to the reference spectra**.**

For the spectrum of QSO J000443- 555044, observe the x values which are the wavelengths to be the upper bound and y as the Flux as the lower bound, the entire set of values will be converted to an array. Considering only a particular range of wavelength where the function is going to be applied which would result in a proper continuum fit for the metal absorption lines.

The Polyfit function which is a numpy function in python and is written as *Numpy.Polyfit*() helps in finding the least square polynomial fit. In other words it finds the best fitting curve to a given set of points by minimizing the sum of squares. It takes in 3 inputs x,y and the polynomial degree and creates and visualizes the data , fitting the several points and final curves. The function returns the coefficient of the polynomials which is used to model the curve to fit the data.

Now using the straight line equation for the array of the best fit lines upon the continuum flux we normalize the given spectra.

$$y = mx + c$$

where m being the slope of the line and c the intercept.

3.2.1.b Normalization

Normalizing an object's flux to the continuum response is very useful if we want to make relative measurements (such as equivalent widths) on a continuum which behaves like a strong function of wavelength. The continuum is measured, and normalized by dividing it with an arbitrary continuum by using:

W,F,fnorm,cont,mode , where W = is the wavelength of the spectrum that is to be normalized, F = Fluxes for spectrum that is to be normalized, which will be replaced by normalized fluxes,Fnorm = optional output normalized spectrum and Cont = Optional output fitted continuum as decided.

All the values are converted from matrix to array to observe the next best fit lines after normalization. Lastly, with the array of the new best fit line of the normalized flux divided by continuum flux we move on to find the Equivalent Width.

3.3 Results:

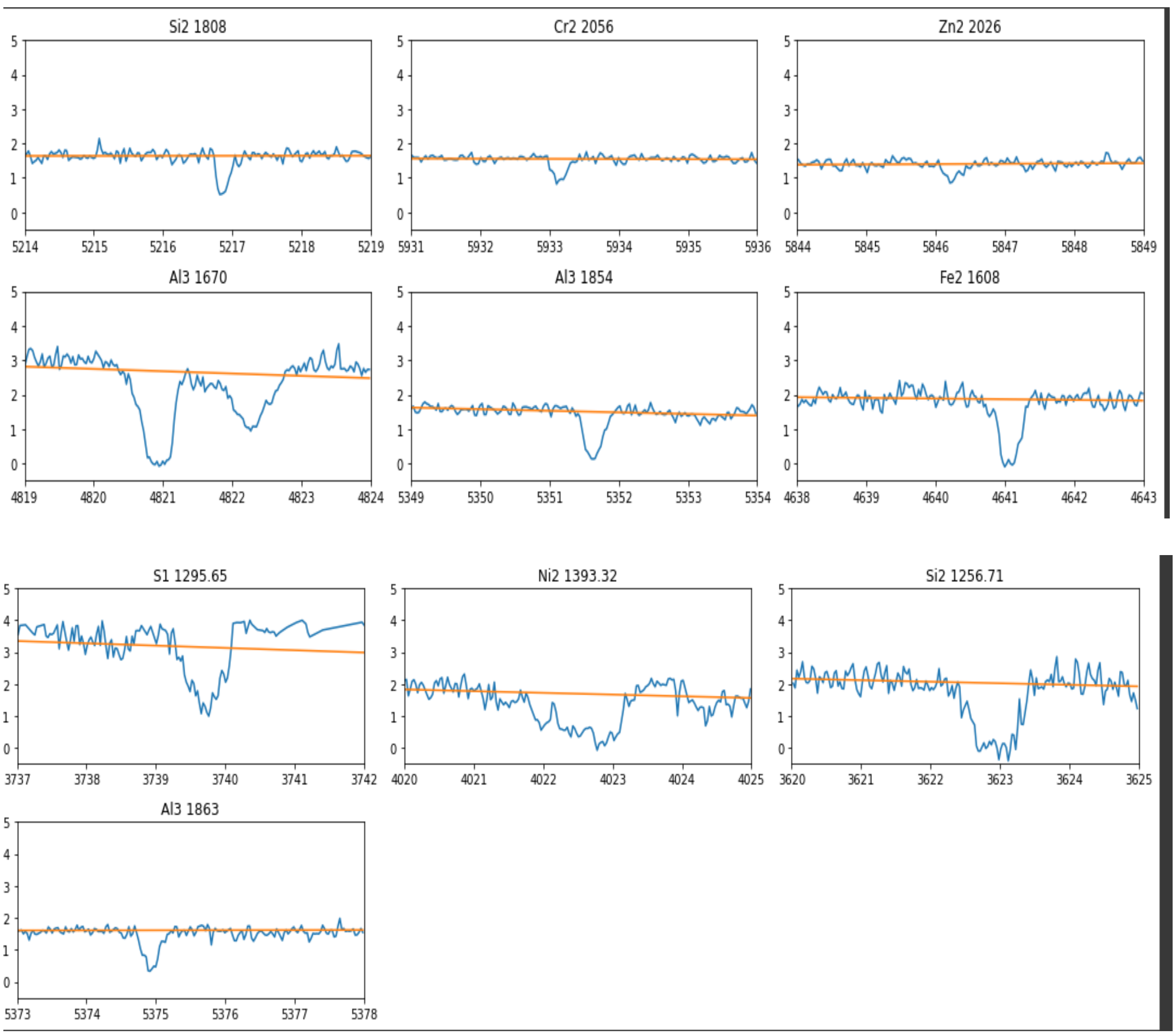

Figure 1.6 Representation of the Un- Normalized Spectrum

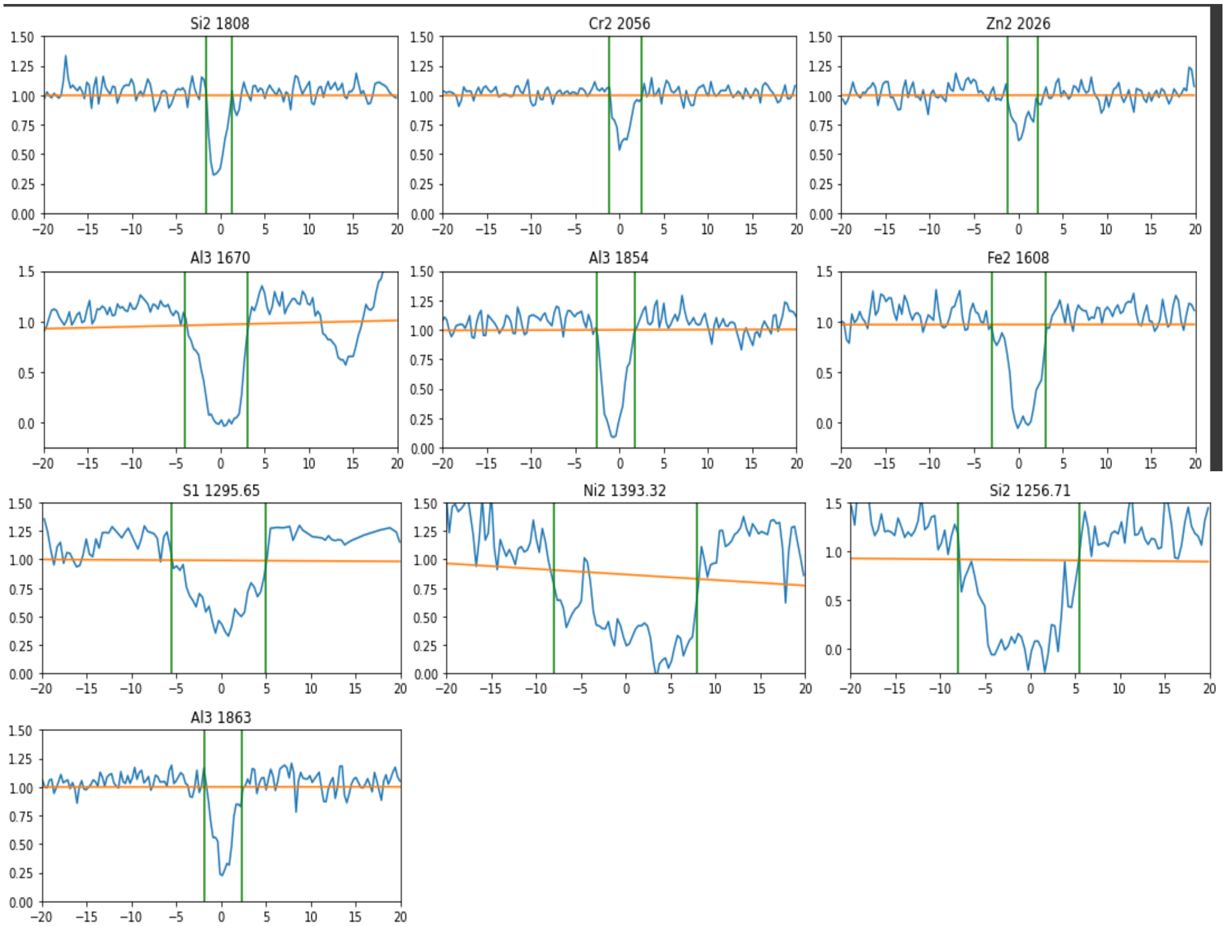

Figure 1.7 : Representation of the observed normalized spectrum

4.Velocity Observation

To observe the velocity of the particular metal absorption lines we need to look into the Doppler's Effect. As the quasars passes through are different amounts of gas clouds which consist of atoms and ions which would absorb certain wavelengths. The redshift would label the wavelength divided by the redshift of the ion. Redshift, or Doppler shift, is the principle where the light waves gets extended towards the red end of the spectrum, which is due to the relative motion of the light source and the observer. Cosmological redshift acts as an important factor in representing the expansion of the universe.

$$z = \frac{\lambda_{obs} - \lambda_{rest}}{\lambda_{rest}}. \quad \text{A.1}$$

Cosmological redshift is related to Dopplers redshift, which results in the distant velocity of the source. Then the Doppler's shift is given by,

$$\lambda_{obs} = \lambda_{rest}\sqrt{\frac{1+\beta}{1-\beta}}, \quad \text{A.2}$$

where, β = (v/c) and v is the apparent recessional speed with respect to the observer. Therefore, for very small recessional velocity, v c, Eq. A.1 can be rewritten as,

$$z = \frac{\lambda_{obs} - \lambda_{rest}}{\lambda_{rest}} = \frac{v}{c}. \quad \text{A.3}$$

Equation A.3 shows that the difference between observed and rest frame is dependent on the velocity(V). Thus, observing the velocity plots plays an important role. In our observation, we have considered a common axis for all the plots to make the comparison of the absorption lines easier.

4.1 Results:

Velocity plots for all the observed Absorption lines.

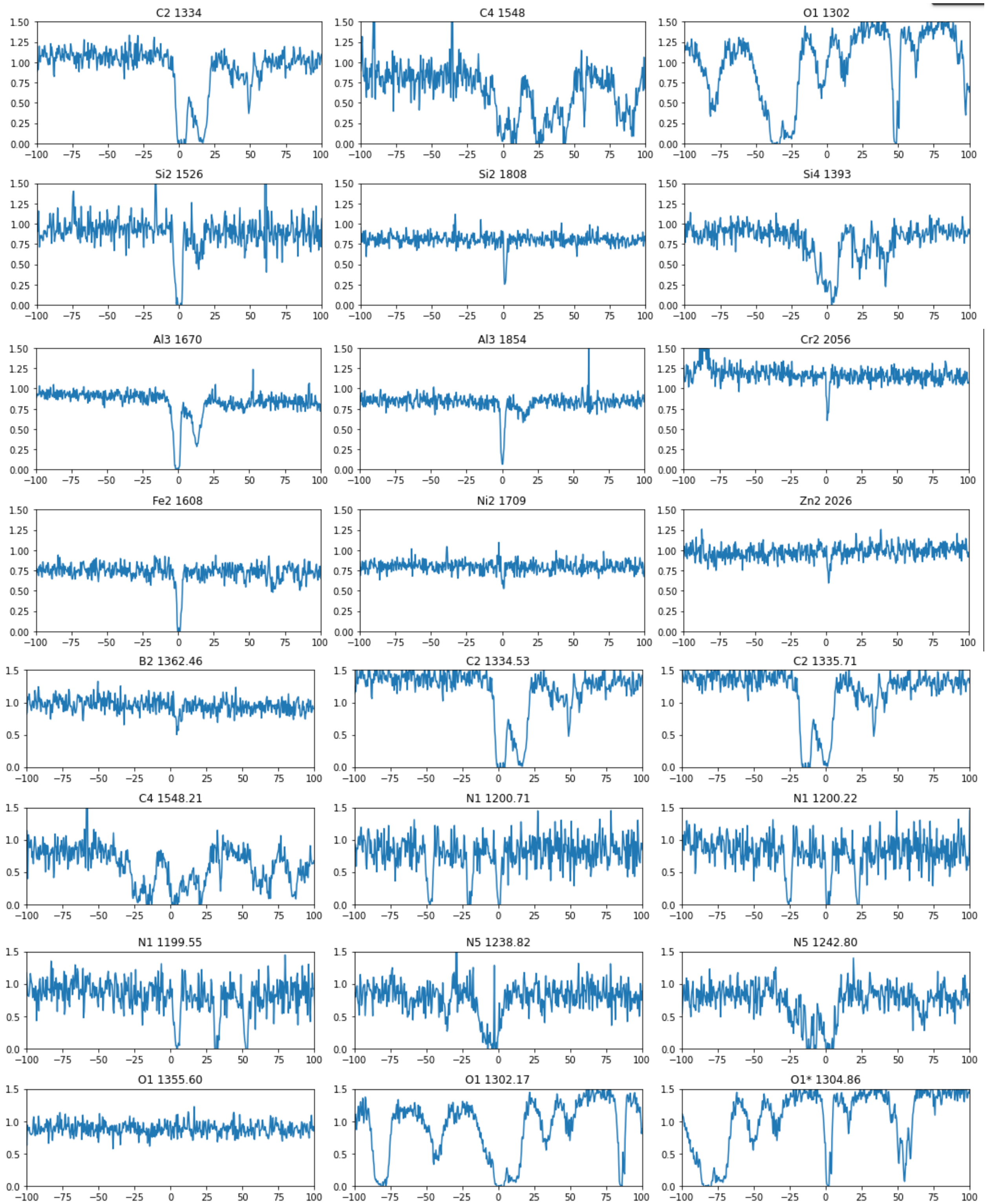

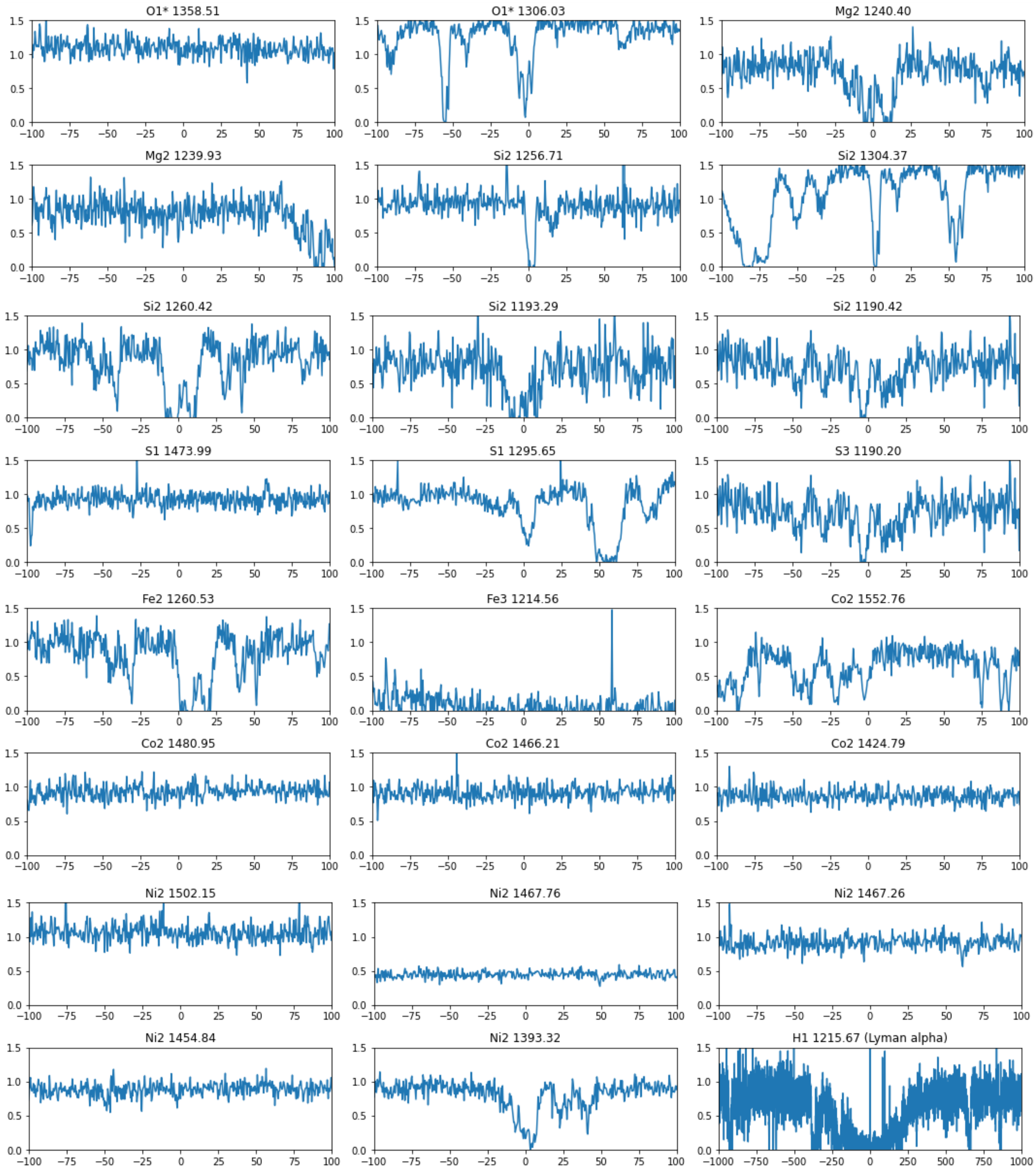

Figure 1.8 : Velocity profile of all the absorption lines observed

4.2 Discussion

From Fig 1.8 we can see that all the dips are at velocity 0 km/sec which indicates that all absorption lines come from the same absorbing cloud. In the case for both the Carbon, Nickel, Silicon we observe that there are multiple dips. This happens if the absorption is taking place through another cloud or there is another line of absorption. Another important reason is due to the oscillatory strength of the absorption lines, which expresses the probability of the absorption or emission of electromagnetic radiation in transition between the energy levels of the atom, which can clearly be observed by finding the Equivalent width (details in chapter 5). For instance the Equivalent Width observed in Al III 1863 and Al III 1854 in (table 1.3). Both belongs to the same ionization state, but Al III 1854 has a broader and stronger absorption profile than the other. As oscillation is concerned with the vibrations of atoms in the molecules so to conclude it can be said that increase in the oscillatory strength is proportional to the increased probability to when a photon will be absorbed.

5.DETERMINATION OF EQUIVALENT WIDTH AND UNCERTAINTY

5.1 Equivalent Width

Equivalent width of a spectral line is measured by the area of the line on the plot of intensity versus wavelength with respect to the continuum level. It's about finding the width and measuring the width within the spectral line. It can easily be derived from an absorption line with no real assumptions. It is a measure of the strength of the spectral features and is expressed as,

The equivalent width, W,

$$W = \int_{\lambda_1}^{\lambda_2} \frac{F_c - F_\lambda}{F_c} \cdot d\lambda, \qquad 6.a$$

Where Fc is the continuum spectral flux and Fλ is the spectral flux on the wavelength of the spectral line.
But, the above integral is replaced by a summation formula and is as follows,

$$W = h_\lambda \cdot \sum_{j=2}^{M-1} \left[1 - \left(\frac{F_j}{F_c}\right)\right], \qquad 6.b$$

Where hλ signifies the spectral dispersion per pixel , (Fj/Fc) represents the relative spectral flux and M represents the number of intervals corresponding to the interval λ.

5.2 Uncertainty on Equivalent Width is calculated

The function in the above equation forms an explicit function of the equivalent width for random quantities of F1, F2. FM and Fc respectively, where Fj and Fc will be considered an independent variable. Fluctuation will be observed, and there will be a possibility of analyzing the error. By using the standard deviation in equation (6.b) ,

$$\left.\frac{\partial W}{\partial F_j}\right|_{\bar{F}_j} = -\frac{h_\lambda}{F_c}, \qquad 6.c$$

Further,

$$\left.\frac{\partial W}{\partial F_c}\right|_{\bar{F}_c} = \frac{1}{\bar{F}_c}(\Delta\lambda - W),$$

$$\text{where } \Delta\lambda = \lambda_1 - \lambda_2. \qquad 6.d$$

From the equation (6.c) and (6.d) we get,

$$\sigma(F_j) = \frac{F_j}{\mathrm{S/N}}, \qquad 6.e$$

Next, the SNR is found out by measuring the continuum pixels and finally we get the uncertainty equation.

$$\sigma_T^2(W) = \left(\frac{h_\lambda}{\mathrm{S/N}}\right)^2 \cdot \sum_{j=1}^{M} \left(\frac{\mathrm{F}_j}{\bar{\mathrm{F}}_c}\right)^2 + \left[\frac{\sigma(\bar{\mathrm{F}}_c)}{\bar{\mathrm{F}}_c}(\Delta\lambda - \mathrm{W})\right]^2.$$

6.f ((A.Chalabaev.et.al(1983)

Uncertainty on equivalent width is calculated.

5.3 Discussions:

Metal Absorption lines	Equivalent Width (Angstroms)	Uncertainty Observed (Angstroms)
Si II 1808	0.136	0.02806000
Cr II 2056	0.100	0.02173567
Fe II 1608	0.371	0.04618482
Al III 1854	0.271	0.034537910
Al III 1863	0.196	0.05257606
Al III 1670	0.534	0.07408294
Zn II 2026	0.096	0.04397588
Ni II 1393	0.883	0.0855816
Si II 1256	0.762	0.08939825

Table 1.3 : Observed equivalent Width

As the equivalent width determines the strength of the absorption line profiles, from table 3 we can observe the strength of the Absorption line profiles. Based on the calculations made these are the observed uncertainties observed, by calculating directly the mean of the errors from the csv file, in finding about the SNR ratio, which is calculated on the continuum pixels.

6.CONCLUSION & FUTURE WORK

6.1 Conclusion

In this work we try to identify the 38-metal line absorption in different transitions. The velocity plots observed in figure 1.7 confirm that all the metal lines observed are from the same spectra. The Equivalent width observed in figure 1.8 shows the abundance of each metal deposition, and determines the strength of the absorption lines.

6.2 Future Work

There are lots to be done for QSO - J000443-555044. Finding the other physical parameters like temperature could be found. We can even investigate the blended lines or determine column densities which is an useful constraint in measuring relative abundances, ionization, excitation or volume densities of the observed absorption lines. Also, here our work is completely based on observational data, but we could also model the same. As we had a limited period of time hence we could not achieve the same.

ACKNOWLEDGEMENTS

I would like to thank all those without whose help and support this work would have not been possible specially my Guide and advisor Dr. Katherine Rawlins for her constant support and encouragement. A special thanks to the Head of Department of Physics of St Xavier's college Mumbai and all the other Faculty and the Lab Assistants for their understanding and constant support. I would also like to thank and dedicate this thesis to my parents for their constant support and motivation which has always helped me accomplish this level, and I will always be thankful to my friends for all their support.

I would also like to express my gratitude towards the European Space Observatory website, from where the data have been taken, which was an important source in carrying out the whole work.

DECLARATION

I declare that the work embodied in the thesis entitled "Spectroscopic analysis of Quasar absorption lines" represents my own contribution to the research carried out under the guidance of Dr Katherine Rawlins from St Xavier's College Mumbai.

The work presented in this thesis has not been submitted for the award of any other degree to this or any other institute. References to other research studies have been duly acknowledged and included in the bibliography.

The thesis has been checked for plagiarism using the software Turnitin, and the soft

A copy of the report is being submitted along with this thesis.

I certify the thesis entitled "Spectroscopic analysis of Quasar absorption lines". submitted by Anamitra Kundu for the award of Master's degree, embodies original work done by him/her under my guidance.

This work has not been submitted to this or any other institute for the award of any other degree.

REFERENCE

[1] Physics of the Interstellar and Intergalactic Medium by Bruce T. Draine (2011)

[2] Sections 5.7, 9.3 of Schneider's text on Extragalactic Astronomy and Cosmology

[3] Katherine Rawlins,[1],[2] Raghunathan Srianand,[3] Gargi Shaw,[4] Hadi Rahmani,5,6 1Department of Physics, University of Mumbai, Santa Cruz East, Mumbai 400 098, India 2UM-DAE Center for Excellence in Basic Sciences, University of Mumbai, Santa Cruz East, Mumbai 400 098, India,[3] Inter-University Center for Astronomy & Astrophysics, Post Bag [4], Ganeshkhind, Pune University Campus, Pune 411 007, India, [4] Tata Institute of Fundamental Research, Homi Bhabha Road, Mumbai 400 005, India " Multicomponent H2 in DLA at zabs = 2.05: physical conditions through observations and numerical models".

[4] Michael T. Murphy,[1], Glenn G. Kacprzak,[1] Giulia A. D. Savorgnan,1 Robert F. Carswell2 "The UVES Spectral Quasar Absorption Database (SQUAD) Data Release 1: The first 10 million seconds. Center for Astrophysics and Supercomputing, Swinburne University of Technology, Hawthorn, Victoria 3122, Australia. Institute of Astronomy, University of Cambridge, Madingley Road, Cambridge, CB3 0HA, UK

[5] ESO science archive.

[6] Eso0120 — Science Release - A Glimpse of the Very Early Universal Web, The VLT Maps Extremely. Distant galaxies.,18th May 2001.
[7] Wolfe, J. M., Horowitz, T. S., & Kenner, N. M. (2005).” Rare items often missed in visual searches” Nature, 435, 439-440.
[8] Chalabaev.A, Maillard,J.P “On the rapid spectral variability of Be-stars : high spectral resolution study of gamma Cas, piPer and 59 Cyg.”Astronomy and Astrophysics, Vol. 127, p. 279-288 (1983